Development 140, 3221-3229 (2013) doi:10.1242/dev.094854

Molecular dissection of IZUMO1, a sperm protein essential for sperm-egg fusion

Naokazu Inoue[1,2], Daizo Hamada[3], Hironari Kamikubo[4], Kunio Hirata[5], Mikio Kataoka[4], Masaki Yamamoto[5], Masahito Ikawa[1], Masaru Okabe[1] and Yoshihisa Hagihara[6,*]

SUMMARY

Although the membrane fusion of spermatozoon and egg cells is the central event of fertilization, the underlying molecular mechanism remains virtually unknown. Gene disruption studies have showed that IZUMO1 on spermatozoon and CD9 on oocyte are essential transmembrane proteins in sperm-egg fusion. In this study, we dissected IZUMO1 protein to determine the domains that were required for the function of sperm-egg fusion. We found that a fragment of the N terminus (Asp5 to Leu113) interacts with fertilization inhibitory antibodies. It also binds to the egg surface and effectively inhibits fusion *in vitro*. We named this fragment 'IZUMO1 putative functional fragment (IZUMO1$_{PFF}$)'. Surprisingly, IZUMO1$_{PPF}$ still maintains binding ability on the egg surface of *Cd9*$^{-/-}$ eggs. A series of biophysical measurements using circular dichroism, sedimentation equilibrium and small angle X-ray scattering revealed that IZUMO1$_{PFF}$ is composed of an N-terminal unfolded structure and a C-terminal ellipsoidal helix dimer. Egg binding and fusion inhibition were not observed in the IZUMO1$_{PFF}$ derivative, which was incapable of helix formation. These findings suggest that the formation of a helical dimer at the N-terminal region of IZUMO1 is required for its function. Cos-7 cells expressing the whole IZUMO1 molecule bound to eggs, and IZUMO1 accumulated at the interface between the two cells, but fusion was not observed. These observations suggest that IZUMO1 alone cannot promote sperm-egg membrane fusion, but it works as a factor that is related to the cellular surface interaction, such as the tethering of the membranes by a helical region corresponding to IZUMO1$_{PFF\text{-}core}$.

KEY WORDS: Sperm-egg fusion, Membrane fusion, IZUMO1

INTRODUCTION

The membrane fusion of spermatozoon and oocyte is the central event of fertilization, where the genetic materials of two gametes merge. Despite the biological importance of this event, targeted deletion studies have revealed only two proteins, CD9 and IZUMO1, to be necessary in sperm-egg fusion (Primakoff and Myles, 2007). Although CD9 is a ubiquitously expressed protein, gene disruption resulted in infertile females but otherwise healthy mice. Subsequent experiments revealed that CD9 functions as an essential factor for sperm-egg fusion in eggs (Kaji et al., 2000; Le Naour et al., 2000; Miyado et al., 2000). We have previously identified a sperm-specific protein, IZUMO1, which is indispensable for mouse sperm-egg fusion (Inoue et al., 2005). In mice lacking either *Cd9* on eggs or *Izumo1* on spermatozoa, membrane fusion was almost completely impaired. To date, how these two proteins mediate membrane fusion is unclear and therefore the molecular mechanism behind of sperm-egg fusion remains virtually unknown.

IZUMO1 is a 377 amino acid type I transmembrane protein with a large extracellular region, a single transmembrane region and a short cytoplasmic tail. In this study, we focused on the 319 amino acid extracellular region of murine IZUMO1. Protein domain search programs (Zdobnov and Apweiler, 2001; McGuffin and Jones, 2003; Letunic et al., 2006) have identified only one immunoglobulin-like domain in the extracellular region. In addition, Ellerman et al. have found that three novel proteins (IZUMO2, IZUMO3 and IZUMO4) share a local sequence similarity with IZUMO1 (Ellerman et al., 2009). These proteins were characterized by the presence of a new sequence motif, called the Izumo domain, with a conserved cluster of eight cysteines: C-X(2)-C-X(106,108)-C-X(3,4)-C-X(9)-C-X(2)-C-X(6)-C-X(4,5)-C. However, it is unclear how these motifs are related to functions of IZUMO1 in sperm-egg fusion.

Here, we have first tried to clarify the functional site in IZUMO1 for sperm-egg fusion by using fusion-inhibiting monoclonal antibodies and a series of recombinant IZUMO1 fragments (Fig. 1). A fluoresceinated fragment that includes the potential functional site was incubated with zona-free eggs and was used to probe its affinity to eggs. In addition, recombinant IZUMO1 fragments were added to the *in vitro* fertilization system and were examined for their fusion inhibitory activities. The biophysical properties of the putative functional site of IZUMO1 were subsequently analyzed using circular dichroism (CD), sedimentation equilibrium and small angle X-ray scattering (SAXS). Combining the above functional and structural data, we discussed the putative molecular function of IZUMO1 in gamete fusion.

MATERIALS AND METHODS

All animal experiments were approved by the Animal Care and Use Committee of the Research Institute for Microbial Diseases, Osaka University, Japan.

Preparation of antibodies

Female rats were immunized with mouse sperm, and spleen cells were subjected to cell fusion with P3U1 cells. Indirect immunofluorescence

[1]Research Institute for Microbial Diseases, Osaka University, Yamadaoka 3-1, Suita, Osaka 565-0871, Japan. [2]Department of Cell Science, Institutes for Biomedical Sciences, School of Medicine, Fukushima Medical University, 1 Hikarigaoka, Fukushima City, Fukushima 960-1295, Japan. [3]Division of Structural Biology (GCOE), Department of Biochemistry and Molecular Biology, Graduate School of Medicine, Kobe University, 7-5-1 Kusunoki-cho, Chuo-ku, Kobe, Hyogo 650-0017, Japan. [4]Graduate School of Materials Science, Nara Institute of Science and Technology, Ikoma, Nara 630-0101, Japan. [5]SPring-8/RIKEN, Kouto, Sayo-gun, Hyogo 679-5148, Japan. [6]National Institute of Advanced Industrial Science and Technology (AIST), 1-8-31 Midorigaoka, Ikeda, Osaka 563-8577, Japan.

*Author for correspondence (hagihara-kappael@aist.go.jp)

Accepted 28 May 2013

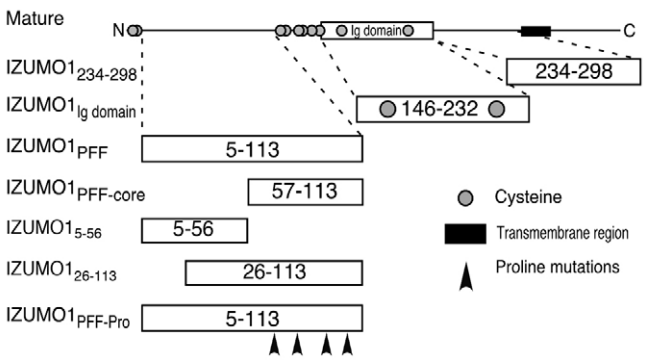

Fig. 1. Mouse mature IZUMO1 and fragments. The region of each fragment is shown by the position of the aligned blank bar, with the N- and C-terminal amino acid residue numbers inside the bar. The N-terminal amino acid sequence of native IZUMO1 was confirmed to be Cys-Ile-Lys-Cys-Asp. The fragments that were used in this work were numbered after the removal of signal peptides (from the first Met to the 21st Pro) from the pre-protein. Gray circles and filled bar in mature IZUMO1 indicate the cysteines and transmembrane region, respectively. There are two clusters of cysteines: at the distal N-terminal end and around residues 114-144. We prepared $IZUMO1_{PFF}$ and $IZUMO1_{PFF\text{-}core}$ with and without a His-tag and linker. In addition, the fragments with an additional cysteine and linker at the C terminus were also made for the conjugation of a fluorescent dye. $IZUMO1_{234\text{-}298}$, $IZUMO1_{5\text{-}56}$ and $IZUMO1_{26\text{-}113}$ have an additional nine amino acids containing a His-tag and linker.

staining as the first screening was employed (Okabe et al., 1987). Hybridomas expressing anti-IZUMO1 antibodies were then further selected by western blotting using a hybridoma culture as a source of primary antibodies. Each hybridoma culture was compared in terms of reactivity against proteins with a molecular weight of 56 kDa in the sperm extract.

Preparation of IZUMO1 fragments

DNA coding for the extracellular region of mouse IZUMO1 was constructed using synthetic DNA with codon use that was optimized for expression in *Escherichia coli*. IZUMO1 fragments were amplified by polymerase chain reaction (PCR) with a 3′-primer with and without sequence encoding Ala-Gly-Gly-His-His-His-His-His-His, a linker plus a hexahistidine tag. In addition, IZUMO1 fragments with the sequence encoding Gly-Gly-Gly-Gly-Ser-Cys were prepared for fluorescent labeling by thiol-maleimide coupling. $IZUMO1_{234\text{-}298}$ was designed to start from Pro233 with a His-tag and linker; however, the purified fragment lacked the first proline, as judged by matrix-assisted laser desorption ionization time-of-flight (MALDI-TOF) mass spectrometry. Amplified PCR products were cloned back into pAED4 (Doering and Matsudaira, 1996). In $IZUMO1_{PFF\text{-}Pro}$, Leu70, Leu81, Leu94 and Leu104 of $IZUMO1_{PFF}$ were mutated to prolines using PCR-based mutagenesis.

All constructs were expressed in *E. coli* strain BL21 (DE3) pLysS (Agilent Technologies, La Jolla, CA). $IZUMO1_{PFF}$ and $IZUMO1_{Ig\ domain}$ were strongly expressed and accumulated in inclusion bodies. Inclusion bodies from 1.6 l of culture medium were suspended in 3 ml of 10 mM Tris-HCl (pH 8.5) and were solubilized by the addition of 3 g of solid guanidine hydrochloride (GdnHCl). These samples were then purified over a Superdex 75 (GE Healthcare, Waukesha, WI) that was pre-equilibrated with 6 M urea in 10 mM Tris-HCl (pH 8.5). $IZUMO1_{234\text{-}298}$, $IZUMO1_{26\text{-}113}$ and $IZUMO1_{5\text{-}56}$ were recovered in the soluble fraction and were purified using a HiTrap metal-chelating column (GE Healthcare). Finally, all samples were purified using reverse-phase chromatography, except $IZUMO1_{234\text{-}298}$ and $IZUMO1_{PFF}$ variants with two or more cysteines. $IZUMO1_{234\text{-}298}$ was further purified by ion exchange chromatography. $IZUMO1_{PFF\text{-}core}$ was prepared from partially purified $IZUMO1_{PFF}$ by limited proteolysis using 1/500 (w/w) proteinase K (Merck KGaA, Darmstadt, Germany) at 10°C for 1.5-2 hours. Proteolyzed fragments were then applied to reverse-phase chromatography for final purification of $IZUMO1_{PFF\text{-}core}$.

MALDI-TOF mass spectrometry confirmed that the molecular weights of purified IZUMO1 fragments were identical to the expected values that were calculated from their amino acid sequences (with an error of ±0.025%). Protein stock concentrations were determined by measuring the absorbance at 280 nm in 6 M GdnHCl, 20 mM sodium phosphate (pH 6.5). Molar extinction coefficients were calculated based on the number of Trp and Tyr residues using the Edelhoch spectral parameters (Edelhoch, 1967) (supplementary material Table S1). In this article, the molar concentrations of IZUMO1 fragments were estimated by assuming that they are monomers in a solution.

Measurements of surface plasmon resonance spectra

The antibodies were immobilized to the CM-5 sensor chip by the amine coupling protocol that was supplied by the manufacturer at 25°C using Biacore 2000 (GE Healthcare). The surface plasmon resonance (SPR) spectra of the IZUMO1 fragments were measured in 10 mM HEPES, 150 mM NaCl, 3 mM EDTA and 0.005% Tween-20 at 20°C, and the bound fragments were washed with 10 mM glycine and 0.5 M NaCl at pH 2.0. All experiments were duplicated.

In vitro fertilization

Mouse spermatozoa were collected from the cauda epididymis and were capacitated *in vitro* for 2 hours in a 200 μl drop of TYH medium that was covered with paraffin oil. B6D2F1 female mice (>8 weeks old) were superovulated with an injection of 5 IU of human chorionic gonadotropin (hCG) 48 hours after a 5 IU injection of equine chorionic gonadotropin (eCG). The eggs were collected from the oviduct 14 hours after the hCG injection. Eggs were placed in a 200 μl drop of TYH medium. These eggs were incubated with 2×10^5 spermatozoa/ml for 2 hours at 37°C in 5% CO_2 with anti-IZUMO1 monoclonal antibodies, and unbound spermatozoa were washed away. Eggs were observed 24 hours after insemination for the two-cell development under a Hoffman modulation contrast microscope.

Sperm-egg fusion assay

B6D2F1 female mice (>8 weeks old) were superovulated with an injection of 5 IU of hCG 48 hours after a 5 IU injection of eCG. The eggs were collected from the oviduct 14 hours after the hCG injection. Eggs were placed in a 200 μl drop of TYH medium. After being freed from cumulus cells with 0.01% (w/v) hyaluronidase, the zona pellucida was removed from mouse eggs using a piezo-manipulator, as previously reported (Yamagata et al., 2002). Zona-free mouse eggs were preloaded with 1 μg/ml Hoechst 33342 (Life Technologies, CA, USA) in TYH medium for 10 minutes and were washed prior to the addition of the spermatozoon. Zona-free eggs were co-incubated with 2×10^5 mouse spermatozoa/ml for 30 minutes at 37°C in 5% CO_2 with and without antibodies or IZUMO1 fragments. After 30 minutes of incubation, the eggs were observed under a fluorescence microscope (UV excitation light) after fixing with 0.25% glutaraldehyde. This procedure enabled staining of only fused sperm nuclei by transferring the dye into spermatozoa after membrane fusion.

Assay for the binding of IZUMO1 fragments to mouse eggs

Mouse zona-free eggs (wild type and $Cd9^{-/-}$) were prepared as above. Eggs were incubated with 3 μM IZUMO1 fragments that were fluoresceinated with Alexa Fluor 546 (Life Technologies) and 1 μg/ml of Hoechst 33342 for 2 hours at 37°C in TYH medium. After the eggs had been washed twice in TYH medium for 5 minutes each, the eggs were observed. For these experiments, especially careful preparation of zona-free eggs was required to avoid the occasional aberrant strong staining of eggs by fluoresceinated fragments. We used an FV-1000 microscope (Olympus, Tokyo, Japan) to obtain the confocal images.

Biophysical measurements

CD spectroscopy was performed using a J-820 spectropolarimeter (Jasco, Tokyo, Japan) with a 1 mm cell at 20°C in 10 mM Tris-HCl (pH 8.5) buffer. CD spectra were measured at protein concentrations of 10 μM, except for $IZUMO1_{Ig\ domain}$, which was measured at 20 μM. Sedimentation equilibrium analysis was carried out with an XLA-90 analytical centrifuge (Beckman Coulter, Fullerton, CA) in 10 mM Tris-HCl (pH 8.5) and 50 mM NaCl. The isoelectric points of $IZUMO1_{PFF}$ and $IZUMO1_{PFF\text{-}core}$ are 5.4 and 7.8,

respectively. To increase the solubility and avoid unintended aggregation, we carried out all biophysical experiments, including SAXS, at pH 8.5, which is slightly more alkaline than the reported pH of uterine fluid (pH 7.9±0.4) (Iritani et al., 1971). The helix formation of $IZUMO1_{PFF}$ and $IZUMO1_{PFF\text{-}core}$ at neutral pH was confirmed by CD measurements in 10 mM potassium phosphate (pH 7.1) and 150 mM NaCl (supplementary material Fig. S1).

Chemical crosslinking

IZUMO1 fragments (100 μM) were incubated with 25 times molar excess of bis(sulfosuccinimidyl) suberate (BS^3) (Thermo Scientific, Waltham, MA) in 0.1 M HEPES buffer (pH 7.5) at room temperature for 30 minutes, and then the reaction was quenched by 25 mM Tris-HCl (pH 8.5). The samples (1 μg) were subjected to sodium dodecyl sulfate PAGE (SDS-PAGE) under reduced conditions with untreated samples as controls. Mouse spermatozoa from the cauda epididymis were solubilized with phosphate-buffered saline (PBS) with 1% n-dodecyl-β-D-maltoside (DDM) and 1% protease inhibitor cocktail (Nacalai Tesque, Kyoto, Japan). Solubilized proteins were centrifuged at 15,000 ***g*** for 30 minutes at 4°C, and the supernatants were treated with 0.1, 0.5 and 1 mM BS^3 for 2 hours on ice. After incubation, the reaction was stopped with 50 mM Tris-HCl (pH 7.4) for 15 minutes at room temperature. The samples were subjected to non-reducing SDS-PAGE followed by western blotting. IZUMO1 protein was detected with IZUMO1 monoclonal antibody.

SAXS measurement

SAXS measurements were carried out at BL-10C, Photon Factory, Tsukuba, Japan (Ueki et al., 1985). The wavelength of X-rays was 1.488 Å, as selected by a Si monochromator. The scattering profiles were collected using an R-Axis VII (Rigaku, Tokyo, Japan) and the circularly averaged intensity was used for further analysis. The sample cell had a path length of 1 mm. SAXS data were measured at 15°C in 50 mM Tris-HCl (pH 8.5). SAXS data of $IZUMO1_{PFF\text{-}core}$ were collected at the protein concentrations of 12.9, 10.4, 7.9, 5.1 and 2.5 mg/ml. As a control, scattering profiles from lysozyme that was dissolved in the same buffer at the protein concentrations of 15.7, 12.6, 9.5, 6.2 and 3.1 mg/ml were also measured.

Calculation of the pair-distance distribution [*p*(r)] function

The raw data of SAXS measurements were initially analyzed by Igor Pro (WaveMetrics, Lake Oswego, OR) to calculate the scattering intensities from protein by subtracting the intensity curve that was obtained for the buffer solution and to correct for the protein concentration dependency. The scattering curves after these corrections were analyzed to compute $p(r)$ functions using the program GNOM (Svergun, 1992). The analysis was performed by changing the approximate d_{max} value, and the value with which the $p(r)$ function fell to a natural minimum was determined as the real d_{max}. Scattering data in the Q range of 0.02 to 0.24 $Å^{-1}$ were used in this calculation.

Culture cell-adhesion assay

The cloned mouse *Izumo1* cDNA was ligated into the mammalian expression vector pCXN-2 and Cos-7 cells were transiently transfected with this vector using lipofectamine LTX (Life Technologies). After 2 days, transfected Cos-7 cells were collected with 10 mM EDTA-PBS, washed three times with PBS, and suspended in TYH medium. Mouse eggs expressing green fluorescent protein (GFP) in the cytosol were obtained from transgenic mice with an enhanced GFP cDNA under the control of a chicken β-actin promoter and cytomegalovirus enhancer (Okabe et al., 1997). Wild-type and GFP-expressing zona-free oocytes were prepared as above and incubated with transfected Cos-7 cells at 37°C in TYH medium. IZUMO1 was stained by Alexa Fluor 546-fluoresceinated anti-IZUMO1 monoclonal antibodies.

RESULTS

Fusion inhibitory antibodies bound to the N-terminal region of IZUMO1

Our previous report indicated that glycosylation was not essential for IZUMO1 function (Inoue et al., 2008). Therefore, we speculated

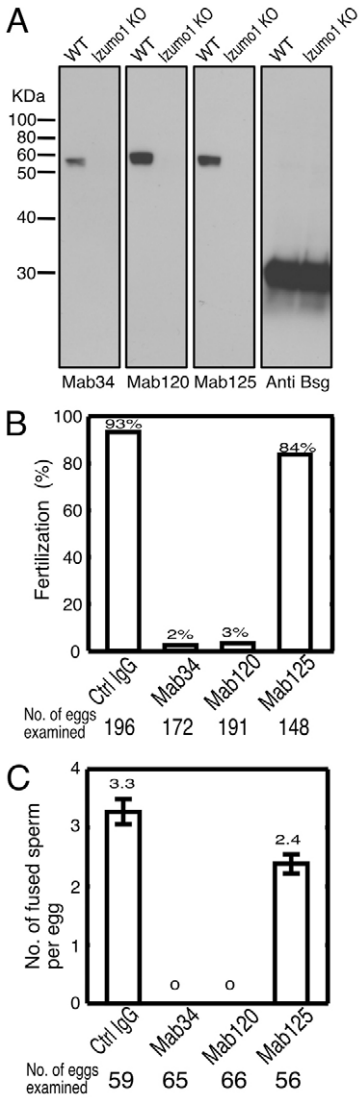

Fig. 2. Establishment of inhibitory monoclonal antibodies to IZUMO1 in sperm-egg fusion *in vitro*. (**A**) All antibodies were immunoreactive against the 56 kDa protein IZUMO1 in wild-type spermatozoa but not in *Izumo1*-null spermatozoa. Solubilized sperm protein (10 μg) was subjected to sodium dodecyl sulfate PAGE (SDS-PAGE), western blotting and detection with anti-IZUMO1 monoclonal antibodies under non-reduced conditions. Basigin (BSG) is shown in the bottom panel as a control. (**B**,**C**) The inhibitory effects of these antibodies were investigated in *in vitro* fertilization and the sperm-egg fusion assay. The *in vitro* fertilization rate was assessed after two-cell development (n=5) (B). Average numbers of fused spermatozoa were observed 30 minutes after insemination (n=3) (C). Total numbers of examined eggs are shown at the bottom of each graph. All analyses were performed in the presence of 10 μg/ml of control IgG, Mab34, Mab120 and Mab125 antibodies. Values are presented as means±s.e.m.

that there must be primary amino acid sequences in IZUMO1 that are important for fusion. We tried to identify the functional site using three new anti-IZUMO1 monoclonal antibodies (Mabs), Mab34, Mab120 and Mab125, which were prepared by immunizing female rats with mouse spermatozoa. In western blot analysis, all of the antibodies detected 56 kDa proteins in wild-type spermatozoa but not in *Izumo1*-null spermatozoa (Fig. 2A), indicating that all of the Mabs are specific for the detection of IZUMO1 in western

blotting. We added these Mabs to an *in vitro* fertilization system and found that only Mab34 and Mab120 significantly inhibited fertilization (Fig. 2B). When the spermatozoa were incubated with zona-free eggs in the presence of these antibodies, the sperm-egg binding was not affected by either of these inhibitory antibodies, but the fusion step was significantly inhibited at a concentration of 10 μg/ml (Mab34 and Mab120) by the sperm-egg fusion assay (Fig. 2C). We measured the concentration dependence of the inhibitory activity of these antibodies, and the inhibition of *in vitro* fertilization was observed even at 0.2 μg/ml of Mab34 and Mab120 (supplementary material Fig. S2).

To search for the functional site of IZUMO1, we separated the sequence of the extracellular region of IZUMO1 into three sections, taking into account the immunoglobulin-like domain. These regions correspond to Asp5-Leu113, Glu146-Leu232 and Pro234-Arg298 (Fig. 1). Of these fragments of IZUMO1, the fusion inhibitory Mabs, Mab34 and Mab120, bound only to the fragment from Asp5 to Leu113, as judged by SPR spectroscopy (Fig. 3A,B). This result indicated that the epitopes of these antibodies are located at the N-terminal region of IZUMO1 (from Asp5 to Leu113) and constitute a putative functional site. We therefore called this fragment 'IZUMO1 putative functional fragment' ($IZUMO1_{PFF}$) (Fig. 1). The dissociation constants of Mab34 and Mab120 were calculated as 1.4 nM (supplementary material Fig. S3A) and 36 nM (supplementary material Fig. S3B), respectively, based on the monomer concentration of $IZUMO1_{PFF}$. Noninhibitory Mab125 recognized $IZUMO1_{234-298}$, which is a proline-rich juxtamembrane region corresponding to the area between the immunoglobulin-like loop and the transmembrane domain (Fig. 3C). OBF13, which is the original anti-IZUMO1 Mab of the IgM class that was reported to inhibit sperm-egg fusion (Okabe et al., 1987; Inoue et al., 2005), also recognized the $IZUMO1_{PFF}$ fragment, albeit weakly (Fig. 3D).

To further scrutinize the antigenic and biophysical properties of $IZUMO1_{PFF}$, we pursued the identification of the structural core of this fragment. Partially purified $IZUMO1_{PFF}$ was incubated with proteinase K at 10°C for 1.5-2 hours, and a major protease-resistant fragment corresponding to residues Val57-Leu113 was recovered by reverse-phase chromatography, suggesting that this fragment folds into a stable structural core. Therefore, we named this fragment $IZUMO1_{PFF\text{-}core}$ (Fig. 1). In addition to this fragment, an N-terminal region of $IZUMO1_{PFF}$ [named $IZUMO1_{5\text{-}56}$ (Asp5-Ala56)] and a short version of $IZUMO1_{PFF}$ lacking the N-terminal 21 amino acid residues [$IZUMO1_{26\text{-}113}$ (His26-Leu113)] were prepared (Fig. 1). None of these short fragments interacted with Mab34 and Mab120 (supplementary material Fig. S4), suggesting that the antibody recognition depends on the tertiary structure of the antigen.

Egg binding and fusion inhibitory activities of IZUMO1 fragments

Because $IZUMO1_{PFF}$ was a candidate for the functional site of sperm-egg fusion, we asked whether it bound to eggs. We produced Alexa Fluor 546-conjugated $IZUMO1_{PFF}$, $IZUMO1_{PFF\text{-}core}$ and $IZUMO1_{5\text{-}56}$ via an additional C-terminal cysteine by thiol-maleimide coupling. These fluoresceinated fragments were incubated with zona-free unfertilized eggs (Fig. 4A-C). The fragments bound to eggs, and the eggs became fluorescent. The

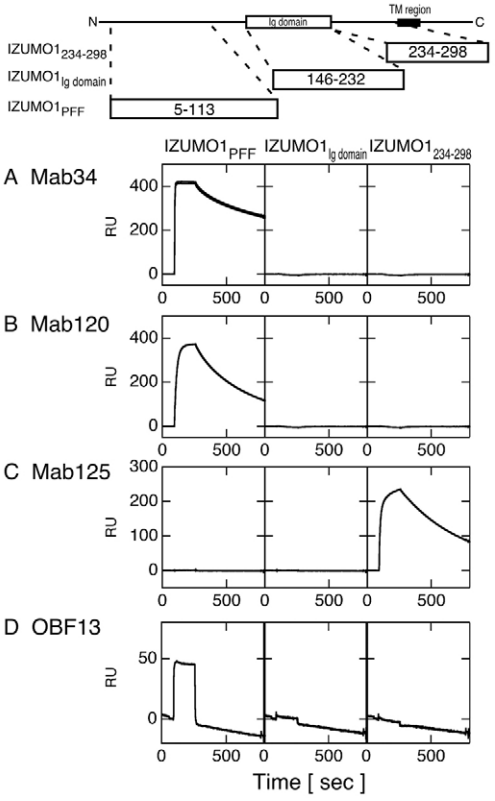

Fig. 3. Interaction of antibodies against the IZUMO1 fragments. (**A-D**) Surface plasmon resonance (SPR) spectra of Mab34 (A), Mab120 (B), Mab125 (C) and OBF13 (D) with 20 μg/ml of $IZUMO1_{PFF}$ (molar concentration is 1.5 μM, assuming the monomer in solution; left panels), $IZUMO1_{Ig\ domain}$ (2.0 μM; middle) and $IZUMO1_{234\text{-}298}$ (2.3 μM; right) were measured.

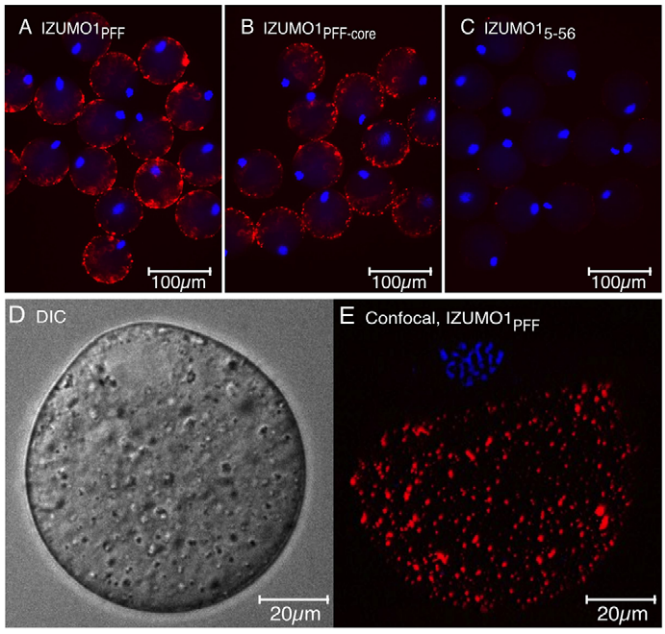

Fig. 4. Binding of IZUMO1 fragments to the egg surface. (**A-C**) The binding of $IZUMO1_{PFF}$ (A), $IZUMO1_{PFF\text{-}core}$ (B) and $IZUMO1_{5\text{-}56}$ (C) to the wild-type egg surface. (**D**,**E**) Differential interference contrast (DIC) (D) and confocal (E) images were taken of the egg with fluoresceinated $IZUMO1_{PFF}$. The egg plasma membrane and nucleus are stained by fluoresceinated IZUMO1 fragments (3 μM) and Hoechst 33342, respectively.

binding of $IZUMO1_{PFF}$ and $IZUMO1_{PFF\text{-}core}$ to eggs was significantly stronger than that of $IZUMO1_{5\text{-}56}$. To investigate precisely the localization of $IZUMO1_{PFF}$ bound on eggs, we acquired differential interference contrast and confocal images of eggs that were incubated with fluoresceinated $IZUMO1_{PFF}$ (Fig. 4D,E). $IZUMO1_{PFF}$ was observed at microvilli-rich regions but not at microvilli-negative regions on the surface of metaphase II chromosomes. The nonuniform distribution of bound $IZUMO1_{PFF}$ suggested that the association between $IZUMO1_{PFF}$ and the egg surface that was observed here was caused by a specific interaction.

Next, we measured sperm-egg fusion in the presence of $IZUMO1_{PFF}$ to ask whether $IZUMO1_{PFF}$ directly affected fertilization (Fig. 5A-C). No significant inhibition was demonstrated by the addition of $IZUMO1_{5\text{-}56}$, $IZUMO1_{PFF\text{-}core}$ and $IZUMO1_{Ig\ domain}$. However, the addition of more than 8 μM $IZUMO1_{PFF}$ significantly inhibited the sperm-egg fusion, and the fusion index (number of spermatozoa that fused to each egg) significantly decreased (Fig. 5C; supplementary material Fig. S5) without affecting sperm motility and egg-binding ability, indicating that the inhibitory effect on fusion occurs during the sperm-egg fusion step and is not based on the sperm-egg binding. These results show that the $IZUMO1_{PFF}$ region is sufficient for both the egg-binding ability and sperm-egg fusion inhibitory activity, and they suggest that this fragment includes the functional site of IZUMO1. In addition, the inhibitory activity of $IZUMO1_{PFF}$ might not come from the saturation of an unknown egg surface receptor for IZUMO1 because $IZUMO1_{PFF\text{-}core}$ bound to eggs but did not prevent the sperm-egg fusion.

$IZUMO1_{PFF}$ bound to the egg surface (Fig. 4) and inhibited sperm-egg fusion *in vitro* (Fig. 5). Therefore, it is plausible that binding partners of IZUMO1 such as CD9 exist on the egg surface. To our surprise, although CD9 is an essential factor for eggs to fuse with spermatozoa, $IZUMO1_{PFF}$ could bind to *Cd9*-null eggs (Fig. 6). Fluoresceinated $IZUMO1_{PFF}$ staining exhibited larger and denser spots than CD9 staining (Fig. 4E) (Inoue et al., 2012). These indicate that there is no physical binding between $IZUMO1_{PFF}$ and

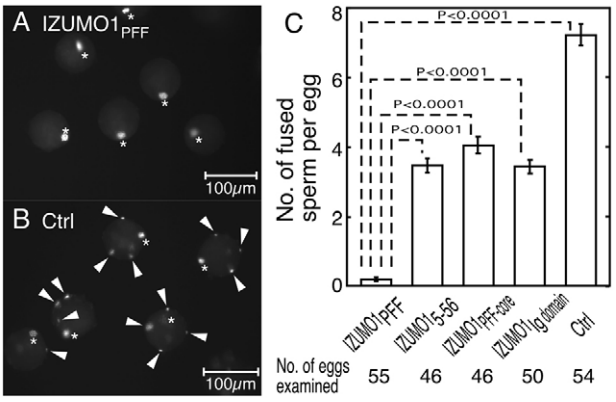

Fig. 5. Effects of IZUMO1 fragments on sperm-egg fusion *in vitro*. (**A**,**B**) The penetration of spermatozoa was examined in the presence of 8 μM $IZUMO1_{PFF}$ (A) and control samples without fragments (B). Fused spermatozoa were stained using Hoechst 33342 that was preloaded into the egg. The arrowheads and asterisks indicate fused spermatozoa and metaphase II-arrested chromosomes, respectively. (**C**) The average number of fused spermatozoa was determined in the presence (8 μM) and absence of fragments. The number of spermatozoa that were fused to an egg was counted using ~50 eggs in each group (n=3). Values are presented as mean±s.e.m.

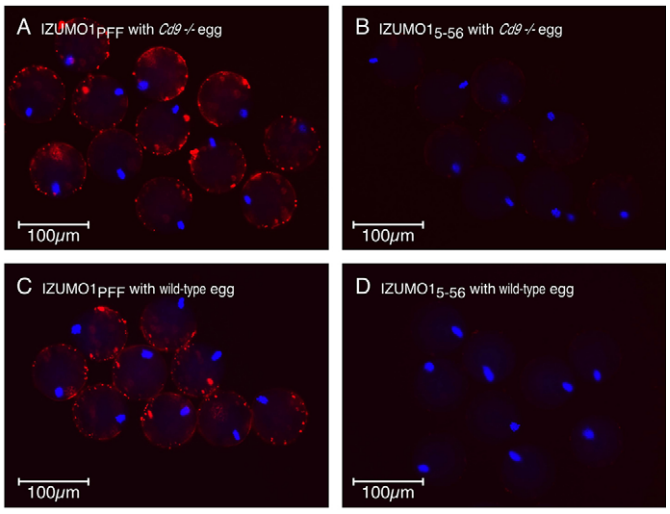

Fig. 6. Interaction of IZUMO1 fragment with *Cd9*$^{-/-}$ egg surface. (**A-D**) Binding of $IZUMO1_{PFF}$ (A,C) and $IZUMO1_{5\text{-}56}$ (B,D) to the *Cd9*$^{-/-}$ (A,B) and wild-type (C,D) egg surface. The eggs were stained with 3 μM Alexa Fluor 546-conjugated IZUMO1 fragments.

CD9. The lack of interaction between $IZUMO1_{PFF}$ and CD9 led us to hypothesize the existence of unknown factors that are involved in gamete fusion. Although CD9-related microvillus formation is considered crucial for fusion, our results suggest that the binding of IZUMO1 to the egg surface may not require a CD9-related strong interaction and/or microvillous formation.

An ellipsoidal helix dimer structure as the putative functional site of IZUMO1

A variety of biophysical analyses of protein solution gives us important information about the structure and size of the target molecule. The CD spectroscopy, which monitors the differences between the absorptions of left-handed and right-handed circularly polarized light, is often used to estimate the contents of secondary structures, as well as to examine whether the target protein is denatured, in combination with equilibrium denaturation experiments. A single measurement of a CD spectrum typically can be carried out with less than 25 μg of protein, which is less protein than required by other biophysical methods. The sedimentation equilibrium is one of the most reliable methods with which to determine the molecular weight and, thus, the oligomeric state of proteins in solution. The method is almost free from nonspecific interactions with carriers and effects of charged residues of proteins that often cause ambiguous interpretations of data from other methods such as gel filtration or electrophoresis without SDS or denaturants. By SAXS measurement, we can obtain information about the distance distribution between each pair of X-ray diffractive atoms, such as carbon and nitrogen, in a protein. Using the SAXS data, the size and low-resolution shape of the protein in solution can be calculated. We believe that the molecular information from such biophysical analysis as mentioned above supplements the results from physiological experiments, which will be helpful in understanding the precise mechanism of sperm-egg fusion.

CD and sedimentation equilibrium analysis revealed that $IZUMO1_{PFF}$ forms a helix dimer (Fig. 7). The limited proteolysis of $IZUMO1_{PFF}$ suggested that $IZUMO1_{PFF\text{-}core}$ is a structural core of the

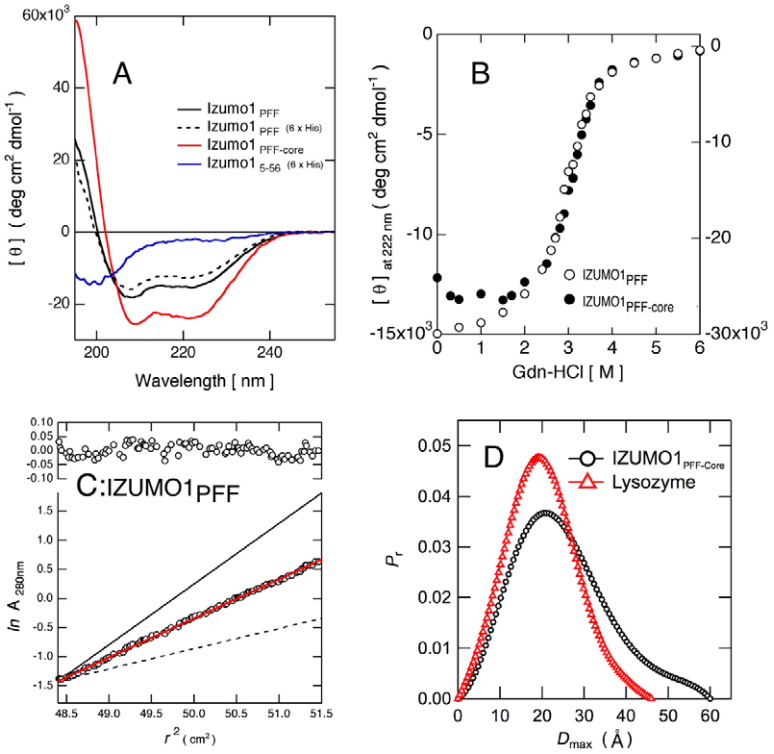

Fig. 7. A series of biophysical measurements of IZUMO1 fragments. (A-D) Circular dichroism (CD) spectra (A), guanidine hydrochloride (GdnHCl)-induced unfolding curves (B), sedimentation equilibrium curves (C) and pair-distance distribution *p(r)* functions (D) of IZUMO1 fragments. (**A**) CD spectra of $IZUMO1_{PFF}$ (black), $IZUMO1_{PFF}$ with His-tag and linker (broken black), $IZUMO1_{PFF\text{-}core}$ (red) and $IZUMO1_{5\text{-}56}$ (blue) were measured For CD measurements, the protein concentration was 10 μM. $IZUMO1_{5\text{-}56}$ has a His-tag and a linker at the C-terminal end. (**B**) The unfolding curves of $IZUMO1_{PFF}$ (open circle) and $IZUMO1_{PFF\text{-}core}$ (closed circle) were detected by ellipticity using a 1 mm cuvette and a protein concentration of 10 μM. The left and right axes are for $IZUMO1_{PFF}$ and $IZUMO1_{PFF\text{-}core}$, respectively. (**C**) Sedimentation equilibrium experiments of $IZUMO1_{PFF}$. The red line is the linear fitting result of the data, indicating that the apparent molecular weight was 25,030. The deviation between the empirical data and the fitted line was plotted in the upper panel. Because the calculated molecular mass of monomeric $IZUMO1_{PFF}$ is 12,916, $IZUMO1_{PFF}$ is predicted to form a dimer. The theoretical lines for a monomer (broken black line) and a trimer (solid black line) are also shown for comparison. The nonlinear fitting analysis gave results that were consistent with those of the linear fitting analysis, in which the differences between these two methods were about 1%. (**D**) *p(r)* functions of $IZUMO1_{PFF\text{-}core}$ (black) and lysozyme (red) were computed by the GNOM program (Svergun, 1992) using their small angle X-ray scattering (SAXS) profiles.

$IZUMO1_{PFF}$ protein. Indeed, $IZUMO1_{PFF\text{-}core}$ exhibited greater negative ellipticity at 222 nm (Fig. 7A). However, the structure of $IZUMO1_{5\text{-}56}$, which is the residual N-terminal region of $IZUMO1_{PFF}$ after $IZUMO1_{PFF\text{-}core}$ is removed, was unfolded, as judged by CD spectroscopy. If the N-terminal region corresponding to $IZUMO1_{5\text{-}56}$ is tightly folded in the context of the whole $IZUMO1_{PFF}$, then $IZUMO1_{PFF}$ should either be more stable than $IZUMO1_{PFF\text{-}core}$ or show a biphasic unfolding transition curve. To examine the stability of both $IZUMO1_{PFF}$ and $IZUMO1_{PFF\text{-}core}$, we tracked ellipticity over a range of GdnHCl-induced unfolding conditions. The midpoint concentrations of unfolding and slopes of transition for both IZUMO1 fragments were identical (Fig. 7B). Combining these data, $IZUMO1_{PFF}$ had a helical structure in its C-terminal region and a mostly unstructured N-terminal region. To assess whether these IZUMO1 fragments formed oligomers, we measured the sedimentation equilibrium profiles at pH 8.5. $IZUMO1_{PFF}$ (Fig. 7C) and $IZUMO1_{PFF\text{-}core}$ (supplementary material Fig. S6A) each exhibited an apparent molecular weight that was 1.9 times its calculated molecular weight, indicating the formation of a dimer in solution, which contrasted with the monomeric characteristic of the $IZUMO1_{Ig\ domain}$ (supplementary material Fig. S6B). The dimerization of $IZUMO1_{PFF}$ and $IZUMO1_{PFF\text{-}core}$ was confirmed by crosslink experiments (supplementary material Fig. S6C). After the reaction of the fragments with the homobifunctional amine-to-amine crosslinker BS^3, we observed decreased monomer fractions and increased dimer fractions by SDS-PAGE of $IZUMO1_{PFF}$ and $IZUMO1_{PFF\text{-}core}$. However, crosslinking is not significant in other fragments. The increased dimeric fraction in the presence of BS^3 was also observed in the intact IZUMO1 in sperm extract (supplementary material Fig. S6D). It is interesting that a small amount of dimeric IZUMO1 can be detected by SDS-PAGE in the absence of BS^3, suggesting that the dimeric structure of intact IZUMO1 is highly stable and that a certain amount of the dimeric form can survive the heat treatment with SDS.

To investigate the molecular shape of $IZUMO1_{PFF\text{-}core}$, we measured the SAXS of both $IZUMO1_{PFF\text{-}core}$ and hen egg white lysozyme as a control because lysozyme has a similar molecular weight to dimeric $IZUMO1_{PFF\text{-}core}$. The $p(r)$ function, which is the probable frequency distribution of all vector lengths between atoms within the scattering particle, can provide information about the shape of the protein molecule. The $p(r)$ function of $IZUMO1_{PFF\text{-}core}$ showed a larger maximum diameter d_{max} (~60 Å) than that of lysozyme (~46 Å) (Fig. 7D). This difference in d_{max} indicates that the structure of $IZUMO1_{PFF\text{-}core}$ is considerably more elongated than that of a typical globular protein such as lysozyme, suggesting that $IZUMO1_{PFF\text{-}core}$ forms an elongated ellipsoidal shape. The presence of a shoulder in the right side of the $p(r)$ function of $IZUMO1_{PFF\text{-}core}$ also supports this idea.

The proline mutant lost egg binding activity and fusion inhibitory activity

Proline is known as a strong helix breaker in aqueous environments (Levitt, 1978). To investigate the functional role of the helix that was identified in the C-terminal region of $IZUMO1_{PFF}$, we prepared a proline mutant of this fragment ($IZUMO1_{PFF\text{-}Pro}$; Fig. 1). As expected, $IZUMO1_{PFF\text{-}Pro}$ lost most of its secondary structure, as shown by CD spectrum (Fig. 8A). The interaction of $IZUMO1_{PFF\text{-}Pro}$ with egg was much weaker than that of $IZUMO1_{PFF}$, but it was similar to that of $IZUMO1_{5\text{-}56}$ (Fig. 8B-D). In addition, no significant fusion inhibitory activity was observed in $IZUMO1_{PFF\text{-}Pro}$ (Fig. 8E). These findings suggested that the helix structure in $IZUMO_{PFF}$ is related to the egg binding and fusion inhibitory effects of $IZUMO1_{PFF}$.

IZUMO1-expressing cultured cells tightly bound egg but did not fuse to egg

To examine whether the IZUMO1 alone can induce the egg binding, which is anticipated from the experiments using $IZUMO1_{PFF}$ and

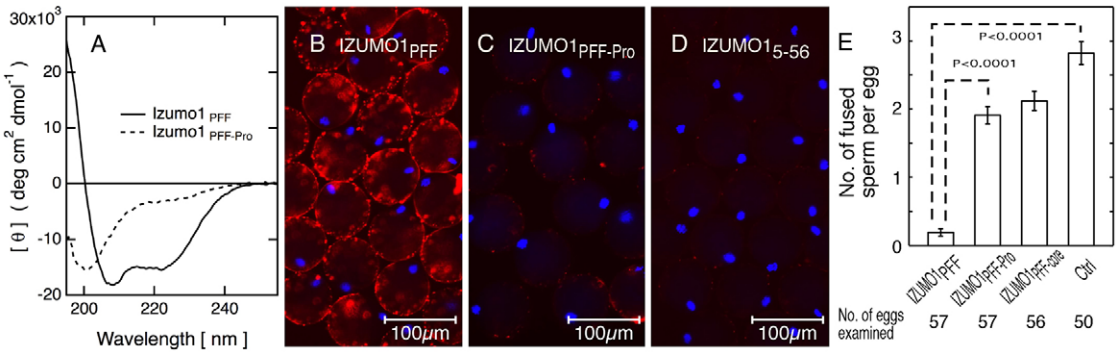

Fig. 8. Influence of helix-breaking mutation on IZUMO1$_{PFF}$. (A-E) Effects of proline mutation on CD spectrum (A), affinity to the egg surface (B-D) and inhibitory activity in sperm-egg fusion *in vitro* (E). (**A**) CD spectra of IZUMO1$_{PFF}$ (black) and IZUMO1$_{PFF\text{-}Pro}$ (broken black line) were measured buffer using a 1 mm cuvette and a protein concentration of 10 μM. (**B-D**) The binding of IZUMO1$_{PFF}$ (B), IZUMO1$_{PFF\text{-}Pro}$ (C) and IZUMO1$_{5\text{-}56}$ (D) to the wild-type egg surface was investigated. The egg plasma membrane and nucleus are stained by fluoresceinated IZUMO1 fragments (3 μM) and Hoechst 33342, respectively. (**E**) The average number of fused spermatozoa in the presence (8 μM) and absence of fragments was calculated. The number of spermatozoa that fused to an egg was counted using ~50 eggs in each group (n=3). Values are presented as mean±s.e.m.

IZUMO1$_{PFF\text{-}core}$, we explored the interaction between egg and recombinant Cos-7 cells that were transfected with the expression vector, including mouse intact *Izumo1* cDNA. After 3 hours of incubation of IZUMO1-expressing Cos-7 cells with wild-type eggs, most of the cultured cells were bound to eggs (Fig. 9). This phenomenon was not observed in Cos-7 cells without IZUMO1 expression. In addition, IZUMO1-expressing cells did not aggregate, indicating that the binding of IZUMO1-expressing Cos-7 cells with eggs is a specific interaction that is mediated by IZUMO1. The fusion of two cells, which was judged by the movement of stained nuclei, did not occur even after 24 hour of incubation. We also confirmed that the cytosol fraction of eggs did not disperse within Cos-7 cells after 24 hours of incubation using the eggs that were obtained from transgenic mice expressing GFP. Fluorescence staining by antibody revealed that IZUMO1 accumulated at the interface between Cos-7 and egg cells (Fig. 9B-D). In addition, Cos-7 cells that were bound to eggs were deformed along the egg surface.

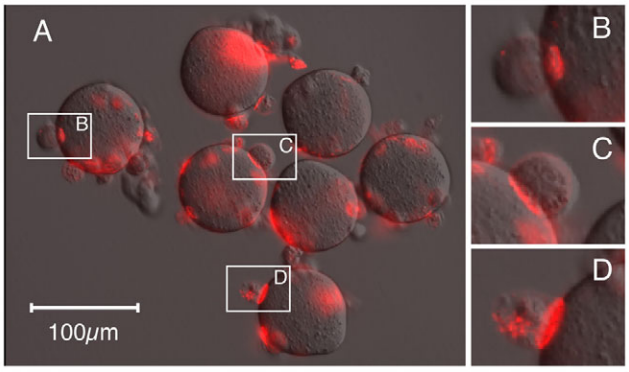

Fig. 9. Interactions between egg and cultured cells transfected with *Izumo1* cDNA. (**A**) Mouse wild-type eggs and Cos-7 cells that were transfected with mouse *Izumo1* cDNA were incubated for 3 hours at 37°C. The fluorescent signal from anti-IZUMO1 monoclonal antibodies that were conjugated with Alexa Fluor 546 was shown in red on the bright-field image. (**B-D**) Magnified image (2.5×) of the region surrounded by the white square in A.

DISCUSSION

In this paper, we have determined that a putative functional site exists in the N-terminal region of IZUMO1. The latter half of this region is important for the binding of IZUMO1 to the egg surface because the fragment corresponding to this part, IZUMO1$_{PFF\text{-}core}$, bound to the egg surface. Although CD9 is an essential factor for sperm-egg fusion in eggs, IZUMO1$_{PPF}$ maintains the binding ability on the egg surface of *Cd9*$^{-/-}$ eggs, indicating that the presence of unknown factors that are related to the gamete fusion. A series of CD, sedimentation equilibrium and SAXS experiments showed that IZUMO1$_{PFF}$ was composed of an N-terminal unfolded region and a C-terminal helix dimer with an ellipsoidal shape. In addition, the IZUMO1$_{PFF}$ mutant, IZUMO1$_{PFF\text{-}Pro}$, which has a defective helical formation, lost egg-binding and fusion inhibitory activities. These results suggest that the formation of a helical dimer at the N-terminal region is essential for the function of IZUMO1.

Recombinant Cos-7 cells expressing whole IZUMO1 did not fuse to eggs. However, we found that these cultured cells bound to eggs and that IZUMO1 accumulated at the interaction site of the two cells. These observations suggest that IZUMO1 alone cannot cause sperm-egg membrane fusion; rather, it induces cellular surface interactions such as membrane tethering. We speculate that the distance between membranes of the spermatozoon and the egg may be not short enough to trigger membrane fusion when IZUMO1$_{PFF}$ binds to the egg surface. Instead, the helical region of IZUMO1 corresponding to IZUMO1$_{PFF\text{-}core}$ may keep the membranes close together. The separation of IZUMO1$_{PFF\text{-}core}$ from the transmembrane region by an immunoglobulin-like domain does not contradict the above notion. There are two examples of essential proteins for fusion, which are supposed to tether membranes. Mitofusin is essential for mitochondrial fusion and forms trans complexes between mitochondria. Mfn1, mammalian mitofusin, forms an antiparallel helix dimer. Because the arrangement of helices is antiparallel and the linker between transmembrane and helical regions is relatively long (>40 amino acids), two membranes that are connected by dimeric mitofusin are distant from each other. Thus, Mfn1 is thought to tether mitochondrial membranes during fusion (Koshiba et al., 2004; Detmer and Chan, 2007). EEA1 is essential for early endosome fusion, and it is proposed to tether endosomes by binding phosphatidylinositol at its C terminus and Rab5 at its N terminus (Christoforidis et al., 1999). The crystal

structure of a C-terminal fragment of EEA1 indicates that a parallel helix bundle is formed next to the phosphatidylinositol-binding FYVE domain. The presence of a strong heptad repeat throughout the sequence suggests that EEA1 forms long, continuous coiled coils and holds two membranes together at a significant distance (Dumas et al., 2001). It should be noted that possible membrane interactions that are induced by IZUMO1 should be different from the binding of spermatozoa around eggs because *Izumo1*-deficient spermatozoa seem to have normal attachments to eggs, but this binding may not facilitate sperm-egg fusion (Inoue et al., 2005). CD9 is also suggested to be involved in membrane adhesion to trigger sperm-egg fusion (Jégou et al., 2011), although spermatozoa bound to *Cd9*-null eggs (Miyado et al., 2000).

Chen and Olson referred to IZUMO1 as a typical non-helix protein that was involved in biological membrane fusion because only the immunoglobulin-like domain can be predicted from the primary sequence as a known structural motif (Chen and Olson, 2005). The β-sheet-rich C2 domain is proposed to induce membrane curvature and to be involved directly in the fusion step (Martens and McMahon, 2008). Because of the similarity between the immunoglobulin-like domain and the C2 domain, fusion-related proteins with immunoglobulin-like domains, including IZUMO1, were hypothesized to work in a similar manner to proteins containing C2 domains, such as synaptotagmin. Our finding requires reconsidering such a view about IZUMO1 and also encourages a search for helix motifs in other proteins that are related to cell-cell membrane fusions, such as myoblast formation, multinucleation of macrophages and epithelial fusion in *Caenorhabditis elegans* (Podbilewicz et al., 2006; Sapir et al., 2007; Helming and Gordon, 2009; Abmayr and Pavlath, 2012).

IZUMO1, IZUMO2, IZUMO3 and IZUMO4 share a novel sequence motif called the Izumo domain, which is characterized by the presence of a conserved cluster of eight cysteines: C-X(2)-C-X(106,108)-C-X(3,4)-C-X(9)-C-X(2)-C-X(6)-C-X(4,5)-C (Ellerman et al., 2009). IZUMO1$_{PFF}$ corresponds to the region between the second and third cysteines. The sequence similarity between IZUMO1 and IZUMO2, IZUMO3 and IZUMO4 is not obvious at this region, where the CLUSTAL W scores were 12.2-15.7 (Thompson et al., 1994). Ellerman et al. observed the dimeric form, in addition to monomeric and trimeric forms, of the Izumo domain of IZUMO1 by SDS-PAGE with mildly denaturing conditions. This is consistent with the data that are presented here. However, they could observe neither the binding of recombinant IZUMO1 fragments, which included the Izumo domain, to the egg nor the inhibitory activity of IZUMO1 fragments on sperm-egg fusion *in vitro*. The discrepancy between our data and those of Ellerman et al. could be explained by the presence of cysteine clusters close to the IZUMO1$_{PFF}$ sequences. These cysteines may affect the structure and negatively regulate the function of IZUMO1. Another possibility is that the cysteines prohibit the correct folding of their recombinant fragments by the aberrant formation of disulfide bonds. Recombinant fragments with those cysteines that were expressed in *E. coli* had intermolecular disulfide bonds under oxidized conditions and thus formed oligomers and aggregates (supplementary material Fig. S7). Although the functional and structural roles of the cysteine cluster are unclear, the IZUMO1$_{PFF}$ fragment was mono-dispersed in solution, had a significant amount of secondary structure, was unfolded cooperatively by a denaturant, exhibited egg-binding activity and inhibited sperm-egg fusion. Furthermore, inhibitory antibodies, which were obtained by the immunization of mouse spermatozoa, recognized the tertiary structure of IZUMO1$_{PFF}$, indicating that our recombinant IZUMO1$_{PFF}$ shares the structure of native IZUMO1. These results strongly suggested the correct and functional folding of our fragment. To uncover the physiological functions of the novel IZUMOs, it will be interesting to study the egg-binding and fusion inhibition activities and structural analysis of fragments of IZUMO2, IZUMO3 and IZUMO4 that correspond to IZUMO1$_{PFF}$.

IZUMO1$_{PFF\text{-}core}$ formed an ellipsoidal dimer, and its helical structure is required for the fusion inhibition and egg-binding activities of this fragment. These features are reminiscent of the known fusion-related proteins such as class 1 viral envelope proteins, SNAREs, mitofusin and EEA1, which consist of a bundle of coiled-coil structures. However, we could not identify an unequivocal coiled-coil region by the prediction programs MultiCoil, LearnCoil and Paircoil2 (Wolf et al., 1997; Singh et al., 1999; McDonnell et al., 2006). The mean residue ellipticity at 222 nm of IZUMO1$_{PFF\text{-}core}$ is larger than the ellipticity that is expected in a typical coiled-coil region (O'Shea et al., 1989), but it is similar to that of the SNARE complex (Fasshauer et al., 1997; Rice et al., 1997). It is fascinating that the machinery in sperm-egg fusion may share the structural motif of a helix bundle with other biological viral and vesicle fusions. A high-resolution structural analysis is required to confirm this hypothesis. We found that IZUMO1 fragments can be crystallized with polyethylene glycol as a precipitant; however, the quality of X-ray diffractions of these crystals was not sufficient to solve the three-dimensional structure. We believe that co-crystallization with an antibody fragment may help improve crystal packing (Koide, 2009).

A function-inhibiting and egg-binding IZUMO1$_{PFF}$, which was identified in this report, will be useful in the search for other components of the egg-fusion machinery. Identifying the essential components of the fusion machinery will greatly assist in the elucidation of the sperm-egg fusion mechanism.

Acknowledgements
We are very grateful to Dr Chris C. Liu at University of Toronto and Dr Adam M. Benham at Durham University for critically analyzing the manuscript and providing valuable advice. We thank Dr Eisuke Mekada and Mr Takao Nishikawa at Osaka University for kindly giving us the *Cd9* disrupted mouse line and for technical assistance, respectively. We also thank Professor Amy E. Keating at Massachusetts Institute of Technology and Professor David C. Chan at California Institute of Technology for their helpful comments on the manuscript.

Funding
This work was supported by grants [19570159 to N.I., K.H., M.Y., Y.H.; 21112006 to N.I.; 21687018 to N.I.] and the Global COE Program A08 from the Ministry of Education, Culture, Sports, Science, and Technology of Japan.

Competing interests statement
The authors declare no competing financial interests.

Author contributions
N.I., M.O. and Y.H. designed research; N.I. performed the experiments using sperm and egg; D.H., H.K. and M.K. performed SAXS studies; M.I. generated antibodies; Y.H. performed the biophysical experiments; K.H. and M.Y. performed structural analysis and crystallographic experiments; N.I., M.O. and Y.H. wrote the manuscript.

Supplementary material
Supplementary material available online at
http://dev.biologists.org/lookup/suppl/doi:10.1242/dev.094854/-/DC1

References
Abmayr, S. M. and Pavlath, G. K. (2012). Myoblast fusion: lessons from flies and mice. *Development* **139**, 641-656.
Chen, E. H. and Olson, E. N. (2005). Unveiling the mechanisms of cell-cell fusion. *Science* **308**, 369-373.

Christoforidis, S., McBride, H. M., Burgoyne, R. D. and Zerial, M. (1999). The Rab5 effector EEA1 is a core component of endosome docking. *Nature* **397**, 621-625.
Detmer, S. A. and Chan, D. C. (2007). Functions and dysfunctions of mitochondrial dynamics. *Nat. Rev. Mol. Cell Biol.* **8**, 870-879.
Doering, D. S. and Matsudaira, P. (1996). Cysteine scanning mutagenesis at 40 of 76 positions in villin headpiece maps the F-actin binding site and structural features of the domain. *Biochemistry* **35**, 12677-12685.
Dumas, J. J., Merithew, E., Sudharshan, E., Rajamani, D., Hayes, S., Lawe, D., Corvera, S. and Lambright, D. G. (2001). Multivalent endosome targeting by homodimeric EEA1. *Mol. Cell* **8**, 947-958.
Edelhoch, H. (1967). Spectroscopic determination of tryptophan and tyrosine in proteins. *Biochemistry* **6**, 1948-1954.
Ellerman, D. A., Pei, J., Gupta, S., Snell, W. J., Myles, D. and Primakoff, P. (2009). Izumo is part of a multiprotein family whose members form large complexes on mammalian sperm. *Mol. Reprod. Dev.* **76**, 1188-1199.
Fasshauer, D., Bruns, D., Shen, B., Jahn, R. and Brünger, A. T. (1997). A structural change occurs upon binding of syntaxin to SNAP-25. *J. Biol. Chem.* **272**, 4582-4590.
Helming, L. and Gordon, S. (2009). Molecular mediators of macrophage fusion. *Trends Cell Biol.* **19**, 514-522.
Inoue, N., Ikawa, M., Isotani, A. and Okabe, M. (2005). The immunoglobulin superfamily protein Izumo is required for sperm to fuse with eggs. *Nature* **434**, 234-238.
Inoue, N., Ikawa, M. and Okabe, M. (2008). Putative sperm fusion protein IZUMO and the role of N-glycosylation. *Biochem. Biophys. Res. Commun.* **377**, 910-914.
Inoue, N., Nishikawa, T., Ikawa, M. and Okabe, M. (2012). Tetraspanin-interacting protein IGSF8 is dispensable for mouse fertility. *Fertil. Steril.* **98**, 465-470.
Iritani, A., Nishikawa, Y., Gomes, W. R. and VanDemark, N. L. (1971). Secretion rates and chemical composition of oviduct and uterine fluids in rabbits. *J. Anim. Sci.* **33**, 829-835.
Jégou, A., Ziyyat, A., Barraud-Lange, V., Perez, E., Wolf, J. P., Pincet, F. and Gourier, C. (2011). CD9 tetraspanin generates fusion competent sites on the egg membrane for mammalian fertilization. *Proc. Natl. Acad. Sci. USA* **108**, 10946-10951.
Kaji, K., Oda, S., Shikano, T., Ohnuki, T., Uematsu, Y., Sakagami, J., Tada, N., Miyazaki, S. and Kudo, A. (2000). The gamete fusion process is defective in eggs of Cd9-deficient mice. *Nat. Genet.* **24**, 279-282.
Koide, S. (2009). Engineering of recombinant crystallization chaperones. *Curr. Opin. Struct. Biol.* **19**, 449-457.
Koshiba, T., Detmer, S. A., Kaiser, J. T., Chen, H., McCaffery, J. M. and Chan, D. C. (2004). Structural basis of mitochondrial tethering by mitofusin complexes. *Science* **305**, 858-862.
Le Naour, F., Rubinstein, E., Jasmin, C., Prenant, M. and Boucheix, C. (2000). Severely reduced female fertility in CD9-deficient mice. *Science* **287**, 319-321.
Letunic, I., Copley, R. R., Pils, B., Pinkert, S., Schultz, J. and Bork, P. (2006). SMART 5: domains in the context of genomes and networks. *Nucleic Acids Res.* **34** Database issue, D257-D260.
Levitt, M. (1978). Conformational preferences of amino acids in globular proteins. *Biochemistry* **17**, 4277-4285.
Martens, S. and McMahon, H. T. (2008). Mechanisms of membrane fusion: disparate players and common principles. *Nat. Rev. Mol. Cell Biol.* **9**, 543-556.
McDonnell, A. V., Jiang, T., Keating, A. E. and Berger, B. (2006). Paircoil2: improved prediction of coiled coils from sequence. *Bioinformatics* **22**, 356-358.
McGuffin, L. J. and Jones, D. T. (2003). Improvement of the GenTHREADER method for genomic fold recognition. *Bioinformatics* **19**, 874-881.
Miyado, K., Yamada, G., Yamada, S., Hasuwa, H., Nakamura, Y., Ryu, F., Suzuki, K., Kosai, K., Inoue, K., Ogura, A. et al. (2000). Requirement of CD9 on the egg plasma membrane for fertilization. *Science* **287**, 321-324.
O'Shea, E. K., Rutkowski, R. and Kim, P. S. (1989). Evidence that the leucine zipper is a coiled coil. *Science* **243**, 538-542.
Okabe, M., Adachi, T., Takada, K., Oda, H., Yagasaki, M., Kohama, Y. and Mimura, T. (1987). Capacitation-related changes in antigen distribution on mouse sperm heads and its relation to fertilization rate in vitro. *J. Reprod. Immunol.* **11**, 91-100.
Okabe, M., Ikawa, M., Kominami, K., Nakanishi, T. and Nishimune, Y. (1997). 'Green mice' as a source of ubiquitous green cells. *FEBS Lett.* **407**, 313-319.
Podbilewicz, B., Leikina, E., Sapir, A., Valansi, C., Suissa, M., Shemer, G. and Chernomordik, L. V. (2006). The C. elegans developmental fusogen EFF-1 mediates homotypic fusion in heterologous cells and in vivo. *Dev. Cell* **11**, 471-481.
Primakoff, P. and Myles, D. G. (2007). Cell-cell membrane fusion during mammalian fertilization. *FEBS Lett.* **581**, 2174-2180.
Rice, L. M., Brennwald, P. and Brünger, A. T. (1997). Formation of a yeast SNARE complex is accompanied by significant structural changes. *FEBS Lett.* **415**, 49-55.
Sapir, A., Choi, J., Leikina, E., Avinoam, O., Valansi, C., Chernomordik, L. V., Newman, A. P. and Podbilewicz, B. (2007). AFF-1, a FOS-1-regulated fusogen, mediates fusion of the anchor cell in C. elegans. *Dev. Cell* **12**, 683-698.
Singh, M., Berger, B. and Kim, P. S. (1999). LearnCoil-VMF: computational evidence for coiled-coil-like motifs in many viral membrane-fusion proteins. *J. Mol. Biol.* **290**, 1031-1041.
Svergun, D. I. (1992). Determination of the regularization parameter in indirect-transform methods using perceptual criteria. *J. Appl. Cryst.* **25**, 495-503.
Thompson, J. D., Higgins, D. G. and Gibson, T. J. (1994). CLUSTAL W: improving the sensitivity of progressive multiple sequence alignment through sequence weighting, position-specific gap penalties and weight matrix choice. *Nucleic Acids Res.* **22**, 4673-4680.
Ueki, T., Hiragi, Y., Kataoka, M., Inoko, Y., Amemiya, Y., Izumi, Y., Tagawa, H. and Muroga, Y. (1985). Aggregation of bovine serum albumin upon cleavage of its disulfide bonds, studied by the time-resolved small-angle X-ray scattering technique with synchrotron radiation. *Biophys. Chem.* **23**, 115-124.
Wolf, E., Kim, P. S. and Berger, B. (1997). MultiCoil: a program for predicting two- and three-stranded coiled coils. *Protein Sci.* **6**, 1179-1189.
Yamagata, K., Nakanishi, T., Ikawa, M., Yamaguchi, R., Moss, S. B. and Okabe, M. (2002). Sperm from the calmegin-deficient mouse have normal abilities for binding and fusion to the egg plasma membrane. *Dev. Biol.* **250**, 348-357.
Zdobnov, E. M. and Apweiler, R. (2001). InterProScan—an integration platform for the signature-recognition methods in InterPro. *Bioinformatics* **17**, 847-848.

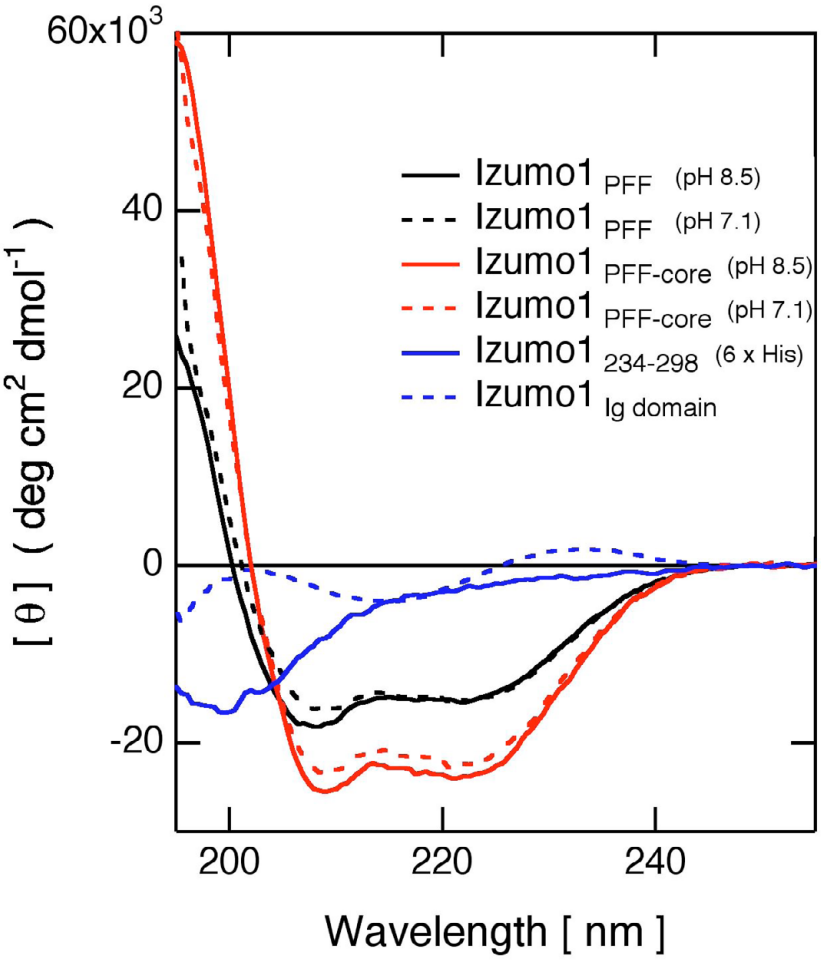

Fig. S1. Circular dichroism (CD) spectra of IZUMO1 fragments. CD spectra of $IZUMO1_{PFF}$ at pH 8.5 (black), $IZUMO1_{PFF}$ at pH 7.1 (broken black), $IZUMO1_{PFF\text{-}core}$ at pH 8.5 (red), $IZUMO1_{PFF\text{-}core}$ at pH 7.1 (broken red), $IZUMO1_{234\text{-}298}$ at pH 8.5 (blue) and $IZUMO1_{Ig\ domain}$ at pH 8.5 (broken blue). For CD measurements, the protein concentration was 10 μM, except $IZUMO1_{Ig\ domain}$ (20 μM).

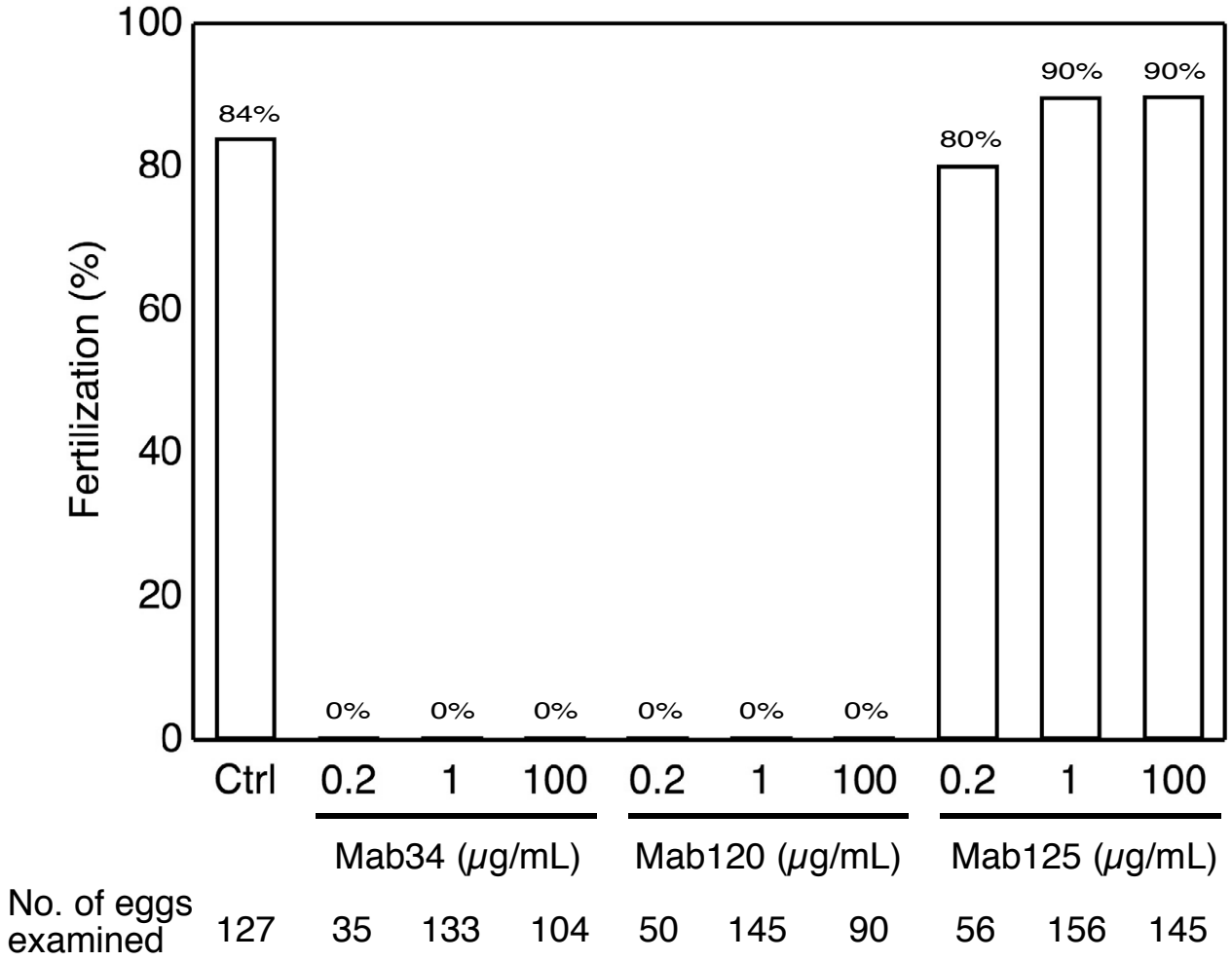

Fig. S2. Concentration dependence of anti-IZUMO1 antibody on the inhibition of *in vitro* fertilization. The average numbers of fused spermatozoa that were observed 30 minutes after insemination were calculated (*n*=3). Analyses were performed in the presence of 0.2, 1 and 100 μg/ml of control IgG, Mab34, Mab120 and Mab125 antibodies.

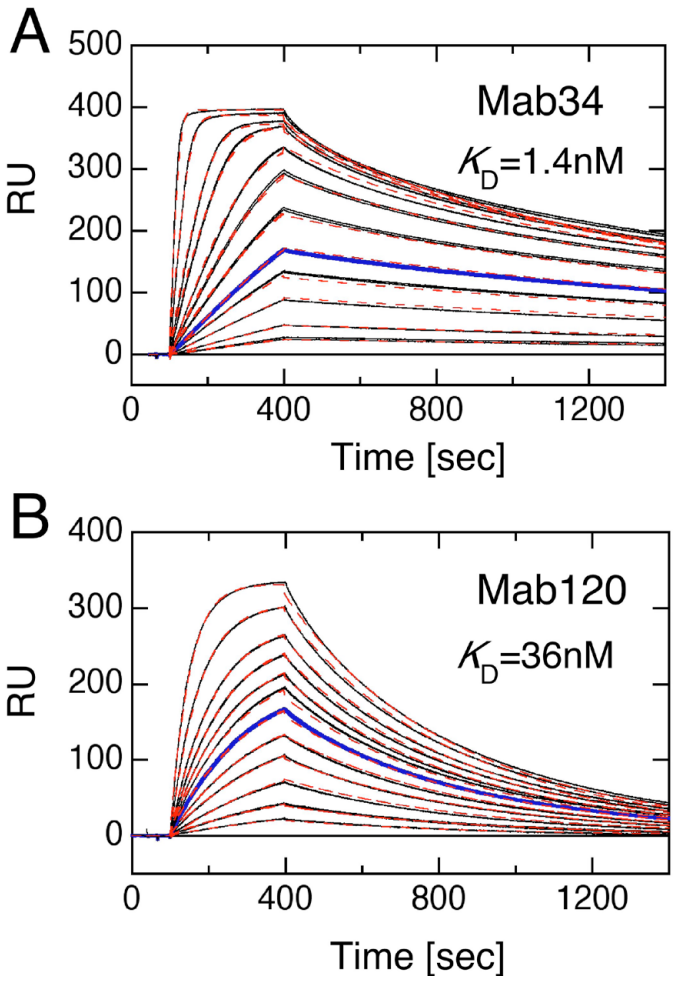

Fig. S3. The surface plasmon resonance (SPR) spectra of immobilized antibodies with various concentrations of IZUMO1$_{PFF}$. (**A**,**B**) To measure Mab34 (A) and Mab120 (B), 11 ng/ml-2 μg/ml and 63 ng/ml-4 μg/ml of IZUMO1$_{PFF}$ were applied to the sensor chips, respectively. The blue lines indicate the empirical sensorgram of 90 ng/ml (7 nM monomer; A) and 640 ng/ml (50 nM monomer; B) of IZUMO1$_{PFF}$, and the black lines show experimental curves at other concentrations of IZUMO1$_{PFF}$. The sensorgrams were analyzed by the global fitting program that was supplied by the manufacturer, and the theoretical curves are shown as broken red lines.

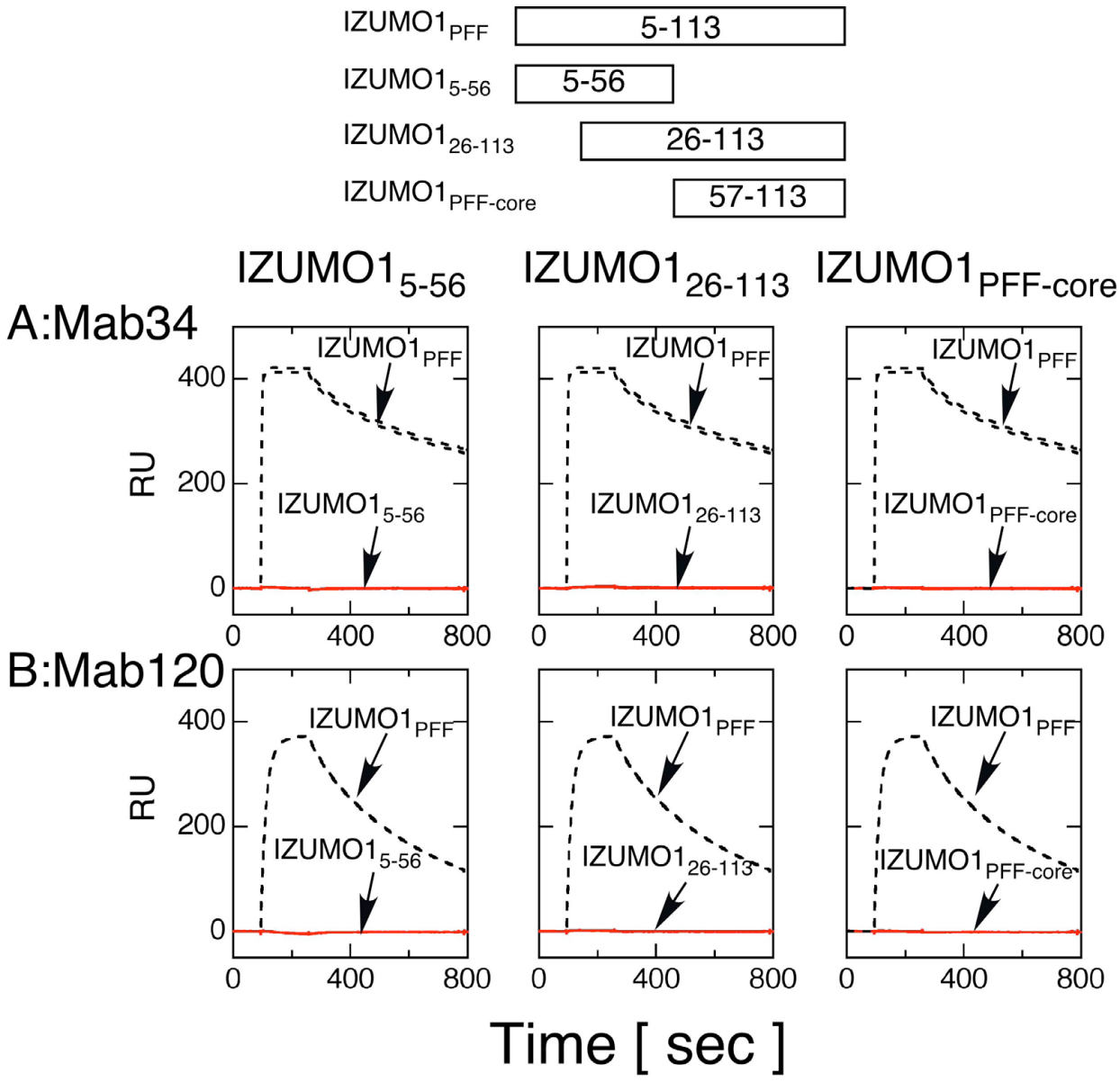

Fig. S4. Interaction of antibodies against IZUMO1 fragments. (**A**,**B**) The SPR spectra of immobilized Mab34 (A) and Mab120 (B) with 20 μg/ml of $IZUMO1_{5\text{-}56}$ (molar concentration is 2.8 μM, assuming the monomer in solution; left panels), $IZUMO1_{26\text{-}113}$ (1.7 μM; middle) and $IZUMO1_{PFF\text{-}core}$ (2.9 μM; right) (red lines). From all of the fragments, only negligible signals were observed compared with $IZUMO1_{PFF}$ (broken black lines).

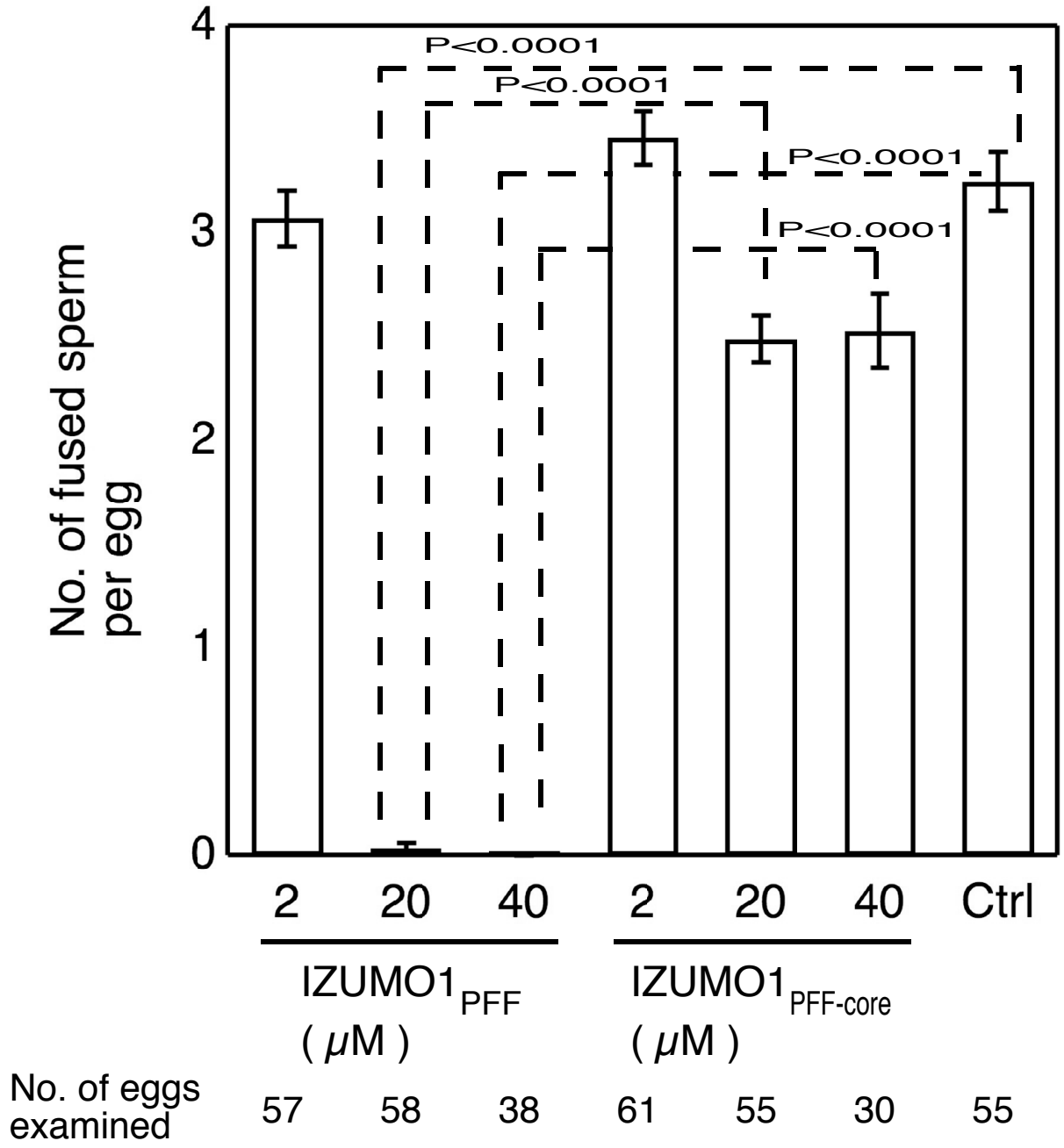

Fig. S5. Concentration dependence of IZUMO1$_{PFF}$ on the inhibition of sperm-egg fusion. The average number of fused spermatozoa in the presence (2, 20 and 40 μM) and absence of IZUMO1$_{PFF}$ was calculated. The number of spermatozoa that fused to an egg was counted using ~50 eggs in each group (n=2). Values are presented as mean±s.e.m.

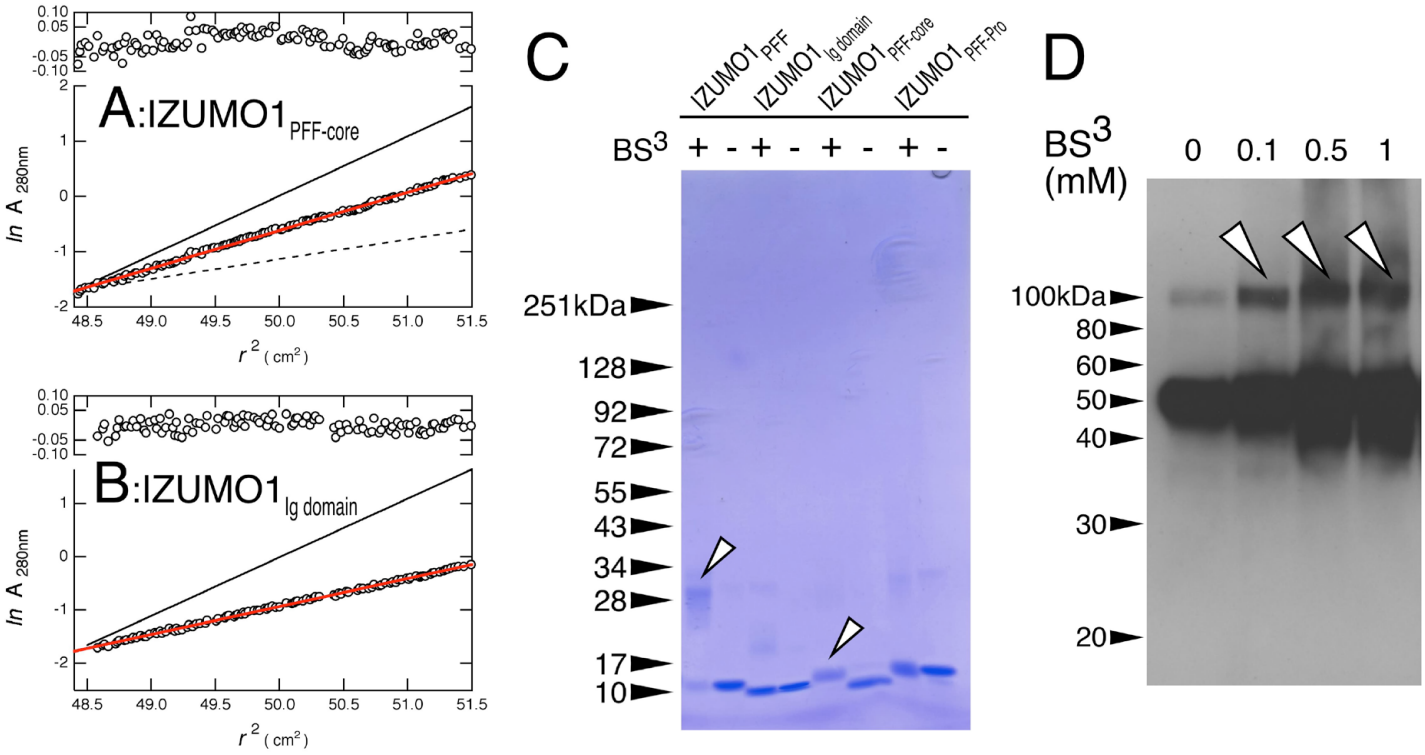

Fig. S6. Sedimentation equilibrium experiments. (**A-D**) IZUMO1$_{PFF\text{-}core}$ (A) and IZUMO1$_{Ig\ domain}$ (B), and chemical crosslinking of IZUMO1 fragments (C) and intact IZUMO1 on sperm (D). (A,B) Red lines are the linear fitting results of the data, indicating that the apparent molecular weights were 13,200 for IZUMO1$_{PFF\text{-}core}$ and 9673 for IZUMO1$_{Ig\ domain}$. The deviation between the empirical data and fitted lines was plotted in the upper panel. The calculated molecular masses of monomeric IZUMO1$_{PFF\text{-}core}$ and IZUMO1$_{Ig\ domain}$ are 6908 and 10,129, respectively. The theoretical lines for the monomer (broken black line in A), dimer (solid black line in B) and trimer (solid black line in A) were shown for comparison. The deviations between molecular weights that were calculated by linear fitting and nonlinear fitting were 1% in both IZUMO1$_{PFF\text{-}core}$ and IZUMO1$_{Ig\ domain}$. (C) IZUMO1$_{PFF}$, IZUMO1$_{Ig\ domain}$, IZUMO1$_{PFF\text{-}core}$ and IZUMO1$_{PFF\text{-}Pro}$ were reacted with a 25 times excess molar amount of a chemical crosslinker, bis(sulfosuccinimidyl) suberate (BS^3), at room temperature and were subjected to sodium dodecyl sulfate polyacrylamide gel electrophoresis (SDS-PAGE) under reduced conditions. Arrowheads indicate bands that correspond to the supposed crosslinked dimer molecule. (D) Solubilized spermatozoa were incubated with a given concentration of BS^3 at 4°C. The samples were analyzed by SDS-PAGE under non-reduced conditions and western blotting carried out using anti-IZUMO1 antibody. The possible crosslinked dimer fractions were shown by arrowheads.

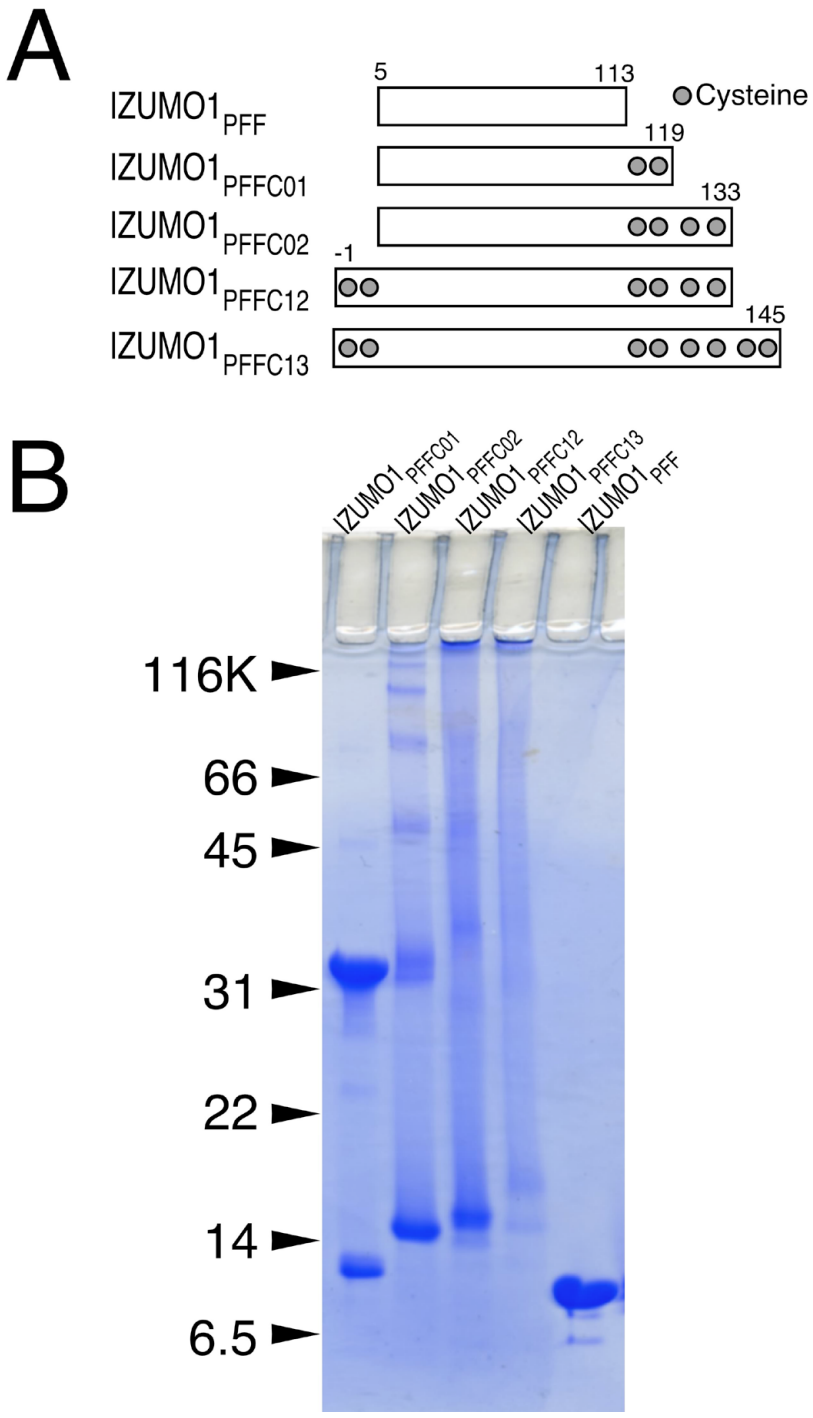

Fig. S7. Aberrant oligomer formation and aggregation of recombinant IZUMO1 fragments with cysteine residues produced by an *Escherichia coli* expression system. (**A**) Schematic representations of IZUMO1 fragments with cysteine clusters found in the IZUMO domain. The positions of cysteines in this cluster are 1, 4, 114, 118, 128, 131, 138 and 144 in mature mouse IZUMO1. (**B**) The refolding and oxidation of IZUMO1 fragments. The samples were subjected to SDS-PAGE under non-reduced conditions.

Table S1. Molar extinction coefficients calculated using the Edelhoch spectral parameters*

Protein	e_{280nm}
$IZUMO1_{Ig\ domain}$	18,020
$IZUMO1_{PFF}$	13,940
$IZUMO1_{234-298}$	2560
$IZUMO1_{PFF-core}$	11,380
$IZUMO1_{5-56}$	2560
$IZUMO1_{26-113}$	12,660
$IZUMO1_{PFF-Pro}$	13,940

*Extinction coefficients of amino acid at 280 nm: Trp, 5690; Tyr, 1280; half cysteine, 120 (Edelhoch, 1967).